THE MIDDLE PLEISTOCENE EXTINCTION OF BATHYAL BENTHIC FORAMINIFERA IN THE SOUTH ATLANTIC (ODP SITES 1082 AND 1088)

A thesis presented in partial fulfilment of the
requirements for the degree of
Master of Science
in
Earth Science

at Massey University,
Palmerston North,
New Zealand

Massey University

Tanya Ann O'Neill

2005

Abstract

The youngest major turnover in deep-sea benthic foraminifera (termed the *Stilostomella* extinction) is documented in two ODP sites in the South Atlantic Ocean. This study is the first detailed investigation of its kind in this region, and reveals the pulsed decline and eventual extinction of 33 species of elongate, cylindrical benthic foraminifera belonging to the families Stilostomellidae, Pleurostomellidae, and part of the Nodosariidae during the mid-Pleistocene climatic transition (MPT, ~1200 – 600 ka). Furthermore, the *Stilostomella* extinction is limited to elongate species with highly specific apertural characteristics (e.g. cribrate, slit lunate, and hooded with secondary teeth), such as *Chrysalogonium*, *Ellipsoglandulina*, and *Pleurostomella* species, respectively.

Micropaleontological and sedimentological data from lower bathyal Sites 1082 and 1088 (1290 m and 2082 m water depth, respectively) provide a proxy record of oceanographic changes in the South Atlantic Ocean through the MPT. This study compares the timing and causes of the *Stilostomella* extinction between two highly contrasting environmental settings in relation to paleoceanographic history, sediment regime and paleoproductivity.

In the South Atlantic, the abundance and accumulation rate of Extinction Group (EG) taxa began to decline between ~1070 and 1000 ka at both core sites. The rate of decline was pulsed, with major declines usually associated with cool periods, and partial recoveries during intervening warm periods. The timing of highest occurrences (HOs) was diachronous between sites, and the final *Stilostomella* extinction datum is marked by the uppermost occurrence of *Myllostomella matanzana* and *Siphonodosaria sagrinensis* at ~705 ka in Site 1082, and *Myllostomella matanzana* and *Pleurostomella alternans* at ~600 ka in Site 1088. This corresponds with the previously documented global *Stilostomella* extinction datum within the period of 700 and 570 ka. Detailed comparisons with North Atlantic and Southwest Pacific studies confirm the highly diachronous nature of HOs of EG species, and furthermore, reveal that there is a lead time of ~100 kyr between HOs of the same species in the North Atlantic, compared with the South Atlantic.

This study suggests that declines and extinctions at Site 1082 were primarily driven by highly fluctuating food supply associated with increased productivity caused by intensified upwelling during MPT glacial periods. In contrast, extinctions at Site 1088 appear to have been a result of the MPT reorganisation of the global deep-water 'conveyor belt', with $\delta^{13}C$ gradients revealing that high dissolved oxygen Glacial North Atlantic Intermediate Water (GNAIW) bathed the region during cool periods. Far from a simple response to change in a single parameter, numerous factors have interacted and appear to have caused the demise of the *Stilostomella* extinction taxa. These factors include encroachment by well-ventilated (high dissolved oxygen) GNAIW, fluctuations in food supply, and possibly winnowing (of the phytodetritus layer) by vigorous bottom currents during MPT glacial periods.

Acknowledgements

I am very grateful to Bruce Hayward for the opportunity to embark on this project, for his enthusiasm, supervision and financial support over the course of this study. I thank the Ocean Drilling Program for providing the samples, isotopic and age model data. A special thanks to the team at Geomarine Research, Hugh Grenfell, Ashwaq Sabaa and Shungo Kawagata, for their hospitality, support and time, which they always so generously bestowed. I would also like to thank those mentioned above for providing data sets from previous *Stilostomella* Extinction studies for very useful comparative purposes, and their suggestions for improving this thesis. Kindest regards to the Hayward household for making me feel so at home!

Thanks to Doug Hopcroft of Hort Research, Palmerston North, for his time and use of the SEM. The supervision of Vince Neall and Julie Palmer was greatly appreciated, as is their unwavering support during my university career. Thank you Vince for your time, encouragement, enthusiasm, our travels, and all the amazing opportunities you have directed my way during the course of my studies. Thanks to all the staff of the Massey University Soil and Earth Sciences Group and postgraduate students. I am especially grateful to Moira Hubbard and Michael Turner for their support and friendship.

Lastly, but most importantly, to my family, I love you and know that without your on-going love and support none of this would have been possible. To my Heavenly Father, for His blessings and grace. Thank you.

Table of Contents

CHAPTER 2 ~ ODP METHODS

CHAPTER 3 ~ METHODS

CHAPTER 4 ~ TAXONOMY

CHAPTER 5 ~ RESULTS

CHAPTER 6 ~ DISCUSSION

List of Figures

List of Tables

List of Plates

Abbreviations and Acronyms

AAIW	Antarctic Intermediate Water
APC	Advanced piston corer
AR	Accumulation rate
B/M	Brunhes/Matuyama paleomagnetic boundary
CC	Core catcher
CCD	Carbonate compensation depth
cos	cosmopolitan
CPDW	Circum Polar Deep Water
DIC	Carbon isotope gradient between intermediate and deep watermasses
DO	Dissolved oxygen
DSDP	Deep Sea Drilling Program
EG	Extinction Group
FI	Fragmentation index
GNAIW	Glacial North Atlantic Intermediate Water
GRA	Gamma-ray attenuation
HO	Highest occurrence
IRD	Ice-rafted debris
lCPDW	lower-Circum Polar Deep Water
LGM	Last Glacial Maximum
lNADW	lower-North Atlantic Deep Water
LOTG	Low-oxygen tolerant Group
LPTM	Late Paleocene Thermal Maximum
MAR	Mass accumulation rate
mbsf	metres below seafloor
mcd	metres composite depth
MIS	Marine Oxygen Isotope Stage
MPT	Middle Pleistocene Climatic Transition
MST	Mulit-sensor track
na	North Atlantic
NADW	North Atlantic Deep Water
NCW	Northern Component Water

NRM	Natural remnant magnetism
ODP	Ocean Drilling Program
%PF	Percent planktic foraminifera
PETM	Paleocene-Eocene Thermal Maximum
PDB	PeeDee Belemnite
psu	Practical Salinity Unit
sa	South Atlantic
SAF	Subantarctic Front
SAMW	Subantarctic Mode Water
SASW	Subantarctic Surface Water
SCW	Southern Component Water
SEM	Scanning electron microscope
SG	Survivor Group
SR	Sedimentation rate
SSSTs	Summer sea-surface temperates
STF	Subtropical Front
swp	South-west Pacific
TOC	Total organic carbon
XCB	Extended core barrel
XRD	X-ray diffraction
uCPDW	upper-Circum Polar Deep Water
uNADW	upper-North Atlantic Deep Water

1. INTRODUCTION

1.1 Objectives

This study is the first high resolution investigation into the *Stilostomella* extinction event in the South Atlantic Ocean. The primary aim of the research was to document the progressive decline, the timing of local disappearances, and the eventual extinction of deep-sea benthic foraminifera in two cores from the South Atlantic Ocean during the mid-Pleistocene Climatic Transition (MPT). This youngest period of benthic foraminiferal extinctions has been attributed to global climate cooling during the MPT between ~ 1200 – 600 ka (Hayward, 2001, 2002; Kawagata *et al.* in press).

Previous studies have revealed that the pulsed decline and extinctions were limited to a specific group of foraminifera, namely, elongate deep-sea foraminifera belonging to the families Stilostomellidae, Pleurostomellidae, and part of the Nodosariidae. Furthermore, the *Stilostomella* extinction selectively affected foraminifera with certain shell morphologies and highly specific apertural characteristics.

South Atlantic ODP Sites 1082 and 1088 have been purposefully chosen to allow for comparisons between two highly contrasting environmental settings, in relation to paleoceanographic history, sediment regime and paleoproductivity. Regional intersite comparisons will be undertaken to investigate whether the timings and causes of the *Stilostomella* extinction were similar at both sites.

Timings of declines and extinctions in the South Atlantic will be compared with proxy data for various environmental factors to provide clues to the cause of these mid-Pleistocene extinctions. Additionally, results will be compared with similar detailed *Stilostomella* extinction studies in the North Atlantic and Southwest Pacific Oceans, in an effort to understand the different timings of highest occurrences in different watermasses (depth) and in different parts of the oceans.

Another aspect to be investigated is the possible link between the morphologic characteristics of the Stilostomella Extinction Group taxa (particularly apertural modifications) and the ordering of highest occurrences both in the South Atlantic and the global scene.

1.2 Southeastern Atlantic Site 1082

1.2.1 Regional Geology

Thirteen sites (1075-1087) were drilled during ODP Leg 175, spanning the western coast of Africa from 5° to 32° S (Fig. 1.1). Site 1082 is located on the Abutment Plateau of the Frio Ridge segment of the Walvis Ridge where it adjoins the continental slope of Namibia. The Walvis Ridge is an aseismic basaltic ridge formed from hotspot activity during the early Cretaceous period (Dean and Gardner, 1985). It extends south-westwards from the continental margin for >2500 km towards the Mid-Atlantic Ridge (Shannon and Nelson, 1996), and may have served as a dam to paleocirculation and current-transported sediment (Bolli *et al.*, 1978), above which thick, mainly biogenic sediment has accumulated.

1.2.2 Location and Modern Oceanographic Setting

ODP Site 1082 (21.5°S, 11.5°E) was drilled during Leg 175 in 1290 m water depth on the Walvis Ridge, c. 250 km offshore from the coast of Namibia. Positioned at the outer edge of the modern Benguela Current Upwelling System (Namibian upwelling cell), the core site is overlain by well-oxygenated, low-salinity Antarctic Intermediate Water (AAIW) (Fig. 1.2), which flows equatorward along the slope off Namibia above which is the Benguela Current (Wefer *et al.*, 1998).

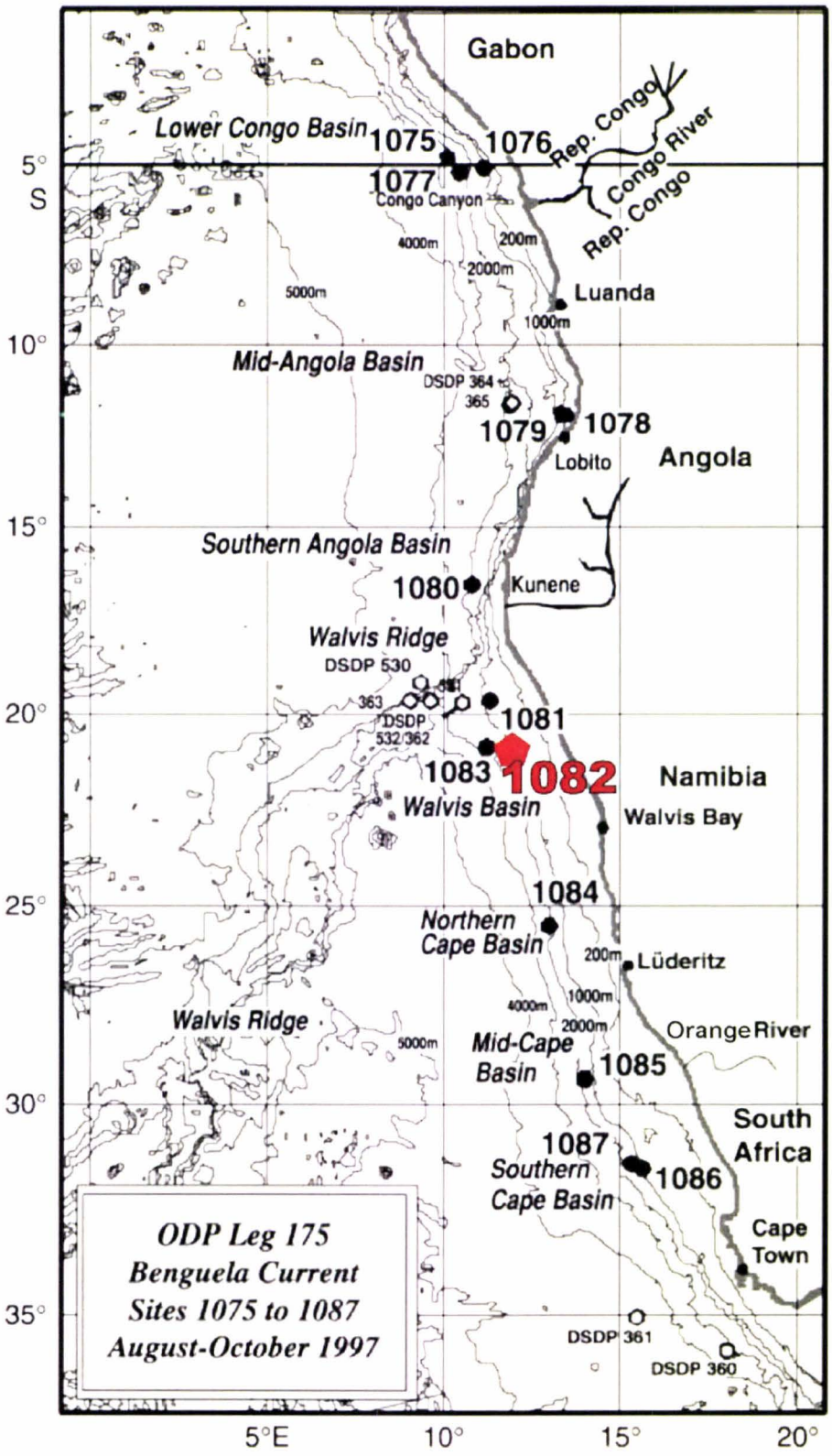

Figure 1.1: Location of Site 1082 in relation to other ODP Leg 175 sites, major bathymetric features and previously drilled ODP and DSDP sites in the South Atlantic study region (modified from Wefer *et al.*, 2001).

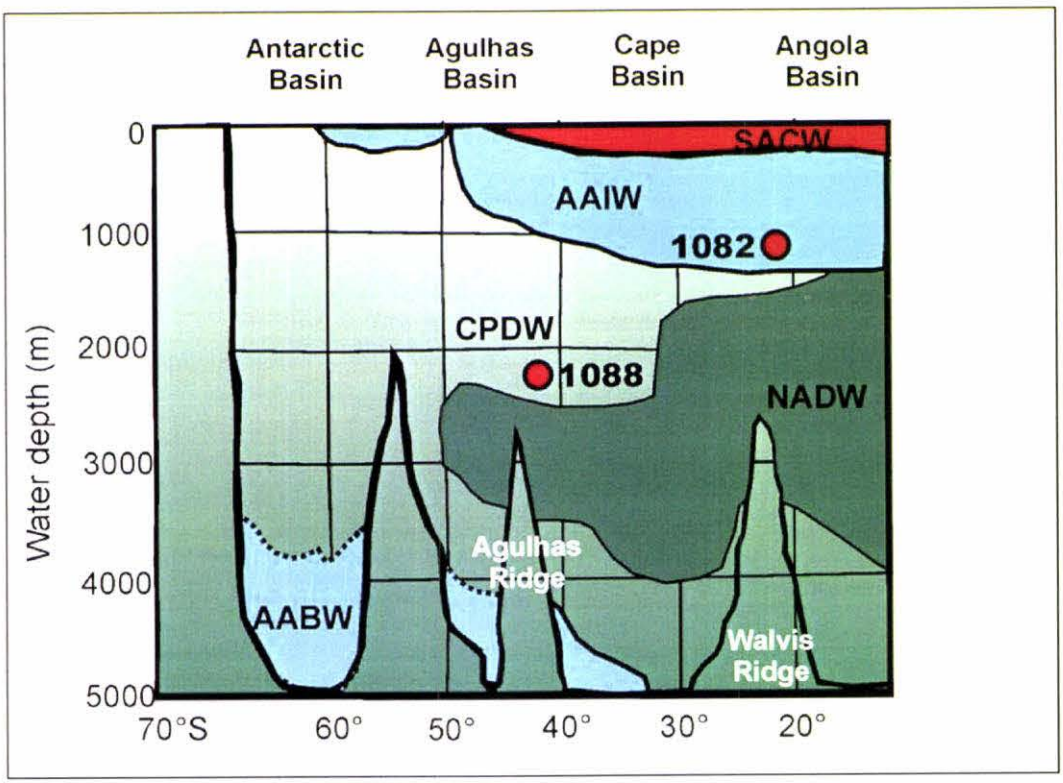

Figure 1.2: A cross-section through the major intermediate- and deep-water masses in the region of Site 1082, South Atlantic Ocean (modified from Gersonde *et al.*, 1999).. AABW = Antarctic Bottom Water; CPDW = Circum-polar Deep Water; NADW = North Atlantic Deep Water; AAIW = Antarctic Intermediate Water; SACW = South Atlantic Central Water.

Modern oceanographic conditions off Southwest Africa have been documented by Moroshkin *et al.* (1970), Bang (1971), Nelson and Hutchings (1983), Shannon (1985a, 1985b), and more recently by Hay and Brock (1992) and Dowsett and Willard (1996). A major component of the heat transfer system from the southeastern Atlantic is the Angola-Benguela Current (ABC) system, comprising the Angola Current and the Benguela Current (Fig. 1.3). The Benguela Current is a shallow (<80 m) equatorward-flowing cool surface current, flowing parallel to and within ~ 320 km off the southwest margin of the African continent (Durham *et al.*, 2001). At ~ 16° S latitude, these northward flowing waters meet the warm and saline southward-flowing Angola Current and develop the Angola-Benguela Front (ABF) (Summerhayes *et al.*, 1995). At this front, the Benguela Current is deflected west and merges with the South Equatorial Current, making up the eastern limb of the South Atlantic Subtropical Gyre. Upwelling of cold, nutrient-rich South Atlantic Central Water (SACW) (from depths between 200-500 m) occurs over the shelf break in response to offshore divergence and along the southwestern African coast in response to offshore Ekman transport (Fig. 1.2). Beneath the SACW lies cold nutrient-rich Antarctic Intermediate Water (AAIW). AAIW is

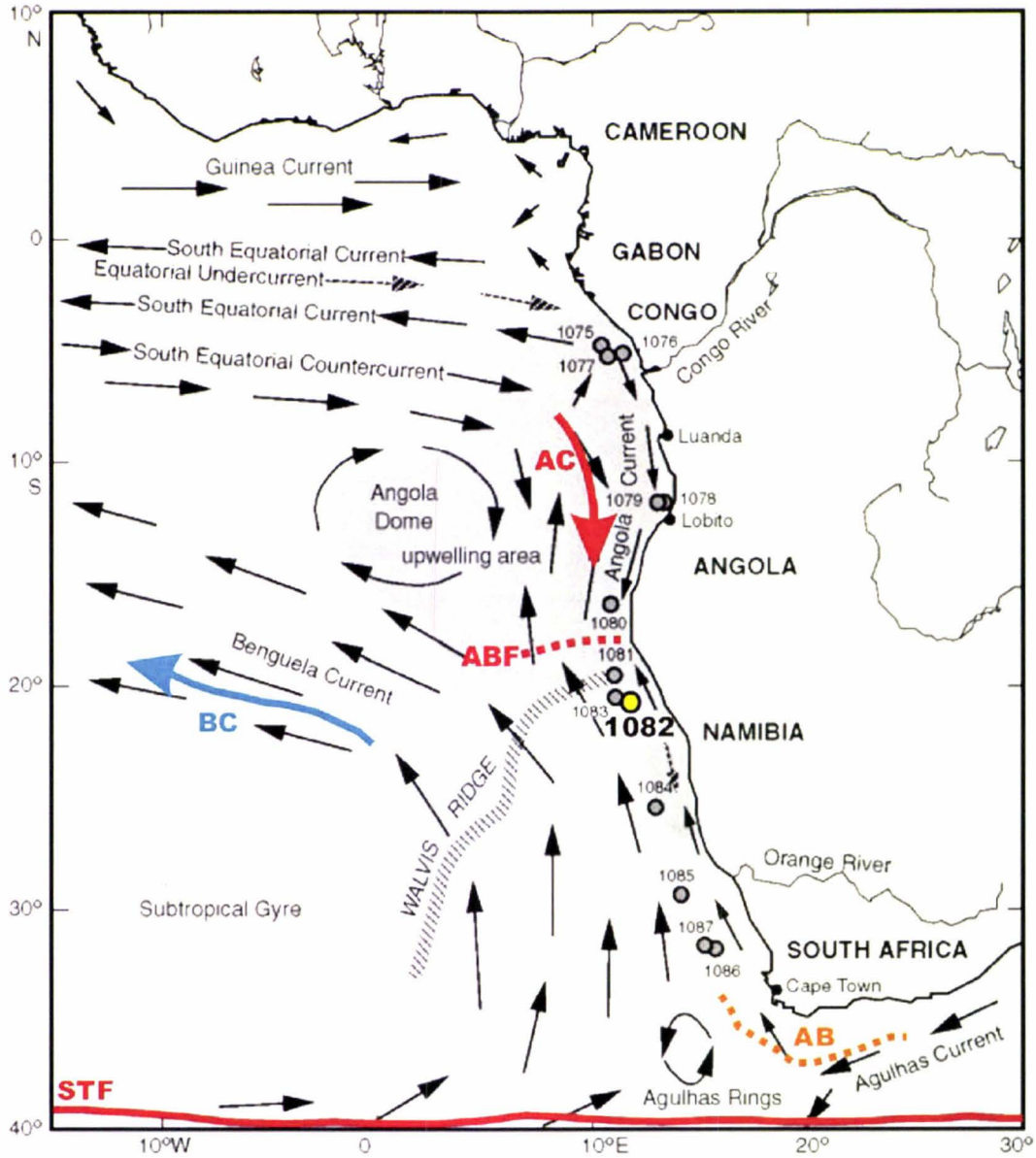

Figure 1.3: Location of ODP Site 1082 and the major surface currents influencing the region today. Arrows represent present day surface currents in the Southeast Atlantic Ocean (modified from Motoyama, 2001). AB = Agulhas Bank; ABF = Angola-Benguela Front; STF = Subtropical Front; AC = Angola Current; BC = Benguela Current.

found in all sectors of the Southern Hemisphere oceans to the north of the Antarctic polar front. Throughout the tropical South Atlantic, AAIW occupies the depth range from 650 to 1050 m (Reid, 1994), with typical temperature and salinity values of 3° C and 34.3 psu, respectively. AAIW spreads across the equator where traces can be found as far north as 30° N in the North Atlantic (Talley, 1996).

The Benguela Current is unusually productive because it delivers an admixture of nutrient-rich AAIW and SACW to the surface through a two-step process (Fig. 1.4)

(Hay and Brock, 1992). Below the surface Benguela Current, a poleward flowing cyclonic subsurface gyre wells up nutrient-rich AAIW (A in Fig. 1.4) to just below the pycnocline, which shoals to less than 250 m off Walvis Bay (Dowsett and Willard, 1996). Here it mixes with the nutrient-rich SACW, and surface upwelling processes, in turn, bring this water up from between 200 m and 330 m to the surface (B in Fig. 1.4), creating a region of cold, nutrient-rich water where primary productivity is very high.

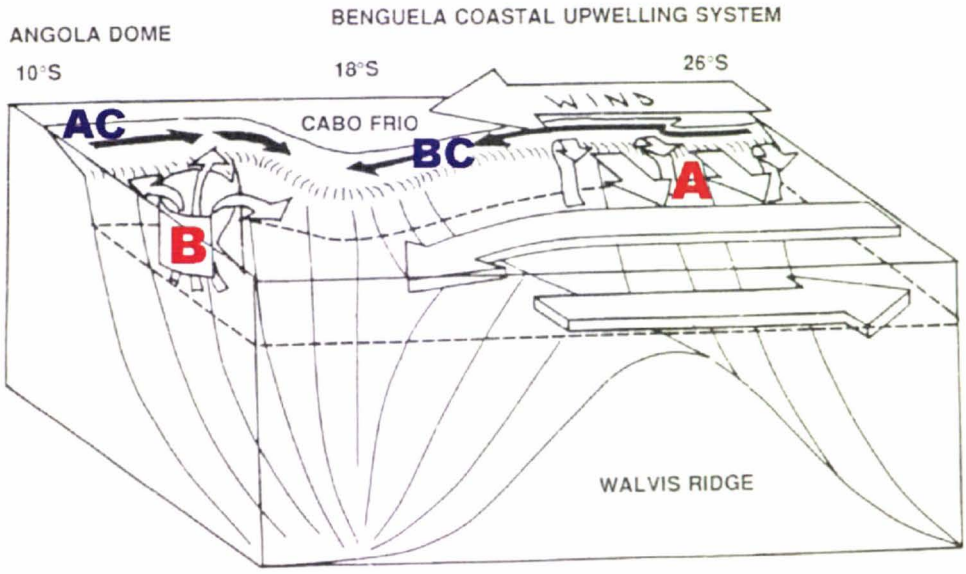

Figure 1.4: Schematic view of the southwest African margin and Walvis Ridge, showing the Angola Current (AC), Benguela Current (BC), coastal upwelling system, and the Angola Dome. Note: A and B refer to upwelling of Antarctic Intermediate Water (AAIW) and South Atlantic Central Water (SACW) (refer to text) (Modified from Hay and Brock, 1992).

Wind conditions along the coast, responsible for the upwelling, are extremely stable because winds circulating around the South Atlantic subtropical high pressure cell are constrained by the steep Kalahari escarpment. The wind stress that intensifies during the Southern Hemisphere summer results in maximum upwelling between December and April each year (Dowsett and Willard, 1996).

To the north, the Benguela Current Upwelling System (BCUS) is bounded, at about 16° S, by the Angola-Benguela Front (ABF) (Fig. 1.3). The ABF migrates seasonally between about 14° S and 16.5° S (Summerhayes *et al.*, 1995). In the late austral summer the front weakens and warm, saline, Angolan water penetrates south along the coast, occasionally reaching 20° S in 'Benguela El Nino' events.

To the south, the BCUS is bounded by the Agulhas Bank (AB in Fig. 1.3), south of which lies the Subtropical Front (STF). This front is known to induce the northward flow of cold filaments of Subantarctic Surface Water (SASW). South of the African coastline and north of the STF warm waters of the Agulhas Current flow in from the Indian Ocean and return east, generating eddies of warm water that spin off to the northwest in the Benguela Current (Summerhayes *et al.*, 1995).

The western margin of the upwelling region is not well defined in terms of sea-surface-temperature anomalies. Satellite imagery has shown large-scale frontal features, resembling 'giant rip-currents', extending up to 500 km offshore (Hay and Brook, 1992).

Present day coastal upwelling varies seasonally, with the seasonal signal more pronounced off Namibia (north of the Orange River) than further south. During the austral winter and spring, water cooler than 16° C extends along the entire coast, but in the summer and autumn its northward extent is reduced. Lutjeharms and Meeuwis (1987) have subdivided the present day Namibian coastal upwelling into four zones or cells, based on the relative strength of the upwelling cell (Fig. 1.5). Their investigations showed upwelling to be particularly strong at ~25° S (centre of the Luderitz upwelling cell), somewhat less so at ~22° S (Walvis cell, ODP Site 1082) and at ~19° S (Namibia cell), and weakest ~17° S (Cunene cell). The Luderitz cell is the coldest, the most persistent, and extends the farthest offshore. Lutjeharms and Meeuwis (1987) also found a strong correlation between intensity of upwelling and the direction and strength of coastal winds. Further, there is also a loose association between the location of upwelling cells and the shape of the seabed, upwelling being more intense where the deep water is closest to the coast (Shannon, 1985). The highest productivity is currently reached off Namibia between 20°S and 25°S. At this latitude optimumal productivity prevails because of the rate of upwelling and the nutrient content of the upwelled waters. Trade winds are strong, offshore transport is vigorous, and cold upwelled water is high in both phosphate and silicate (Wefer *et al.*, 2001).

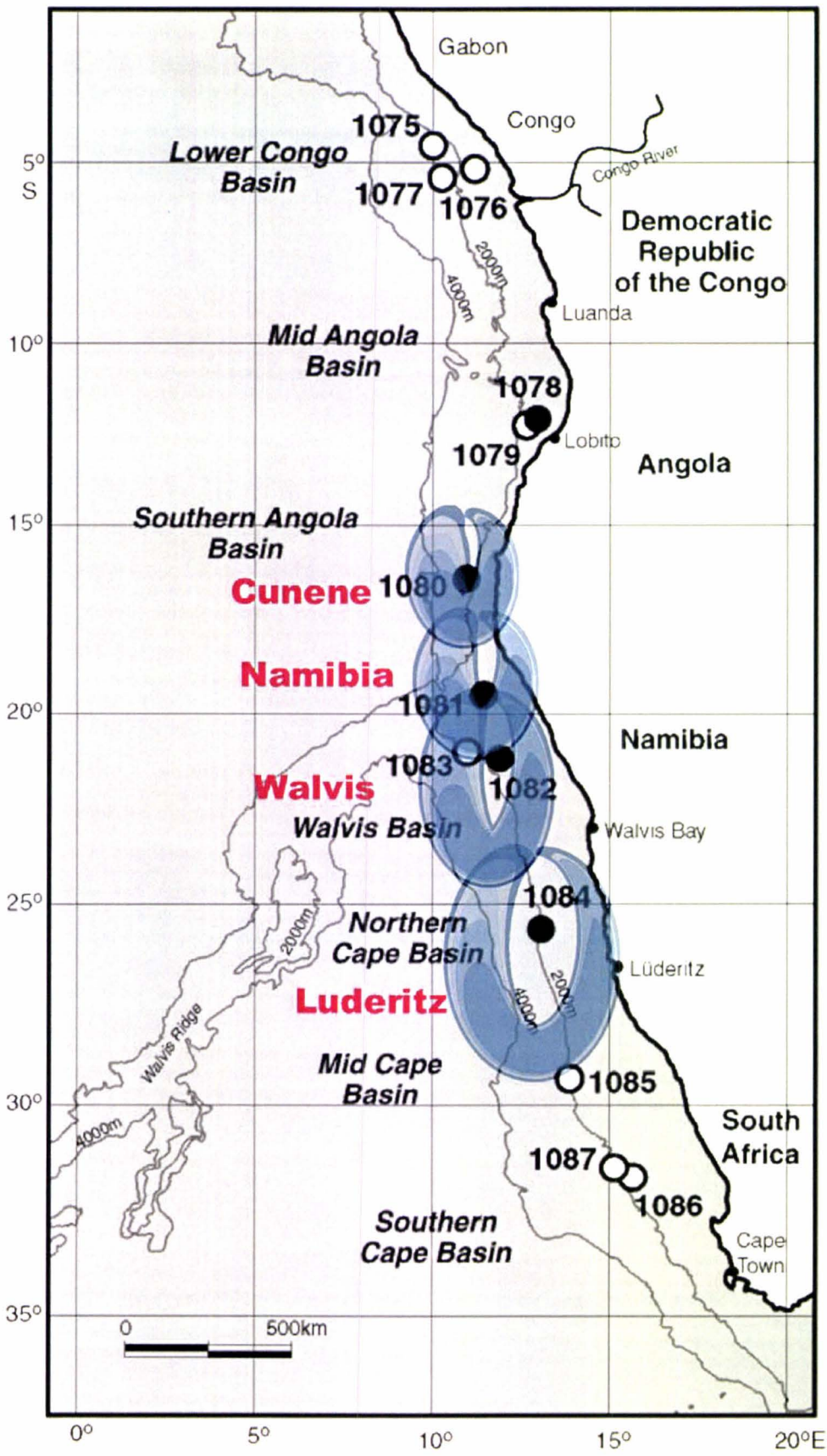

Figure 1.5: Locations of Benguela Current Upwelling System Cells (Modified from Wefer *et al.*, 2001). Note: The size of the upwelling cell is based on its relative upwelling strength.

1.2.3 Past changes in Benguela Current Upwelling System

Previous evidence from the region of the Walvis Ridge has proved to be contentious over the issue of glacial-interglacial upwelling intensity changes, and has been debated by several authors. Studies by Oberhansli (1991), Summerhayes *et al.* (1995) and Little *et al.* (1997) concluded that upwelling at the latitude of the Walvis Ridge generally increased during glacial periods, conversely, other studies suggest that intensity increased during interglacial periods (Diester-Haass, 1985). It has since been suggested, however, that the discrepancy between these studies may in fact be due to the complexity of the site, resulting from past changes in thermohaline circulation, and poor preservation of upwelling indicators (Durham *et al.*, 2001).

Productivity records from nearby Site 1081 (also on the Walvis Ridge) generally provide evidence for increased productivity during glacial intervals, particularly prior to ~1000 ka (Durham *et al.*, 2001). The Mid-Pleistocene Transition (MPT) and associated increased cooling and aridity on the adjacent landmass, brought about changes in the chemical and physical properties of the upwelling water masses and their nutrient content. Durham *et al.*'s 2001 study revealed a significant and rapid drop in overall productivity at ~800 ka. Between 800 and 500 ka productivity began to increase again, however, this was followed by another rapid decrease in productivity at ~500 ka. Post-500 ka fluctuations in productivity were common, with short-lived peaks in response to (1) nutrient-enriched bottom waters being closer to the surface due to sea-level drop and (2) less volume of water in which nutrients were distributed (Hay and Brock, 1992). These peaks were short-lived as enhanced productivity removed nutrients faster than they could be replaced, and consequently, the system stabilized, and productivity decreased once again.

During the Last Glacial Maximum (LGM) the 7° of latitude northward displacement of the Polar Front (PF), the 2° northward displacement of the STF, and the 2-5° C cooling of the Subantarctic Surface Waters, all suggest that the thermal gradient south of Africa steepened in glacial intervals, displacing the South Atlantic mid-latitude high pressure cell north by 2-5° of latitude (Tyson, 1986). The equatorward movement of the pressure system forced a similar shift in the upwelling-favourable Trade Winds, with the steeper thermal gradient also strengthening them. This strengthening of the coastal and shelf-

edge wind field is thereby thought to have enhanced upwelling (intensity and increased productivity) along the Namibian margin during glacial and cooler interstadial periods.

Productivity records from past studies in the region of Site 1082 show that there may not necessarily be a simple response to apparently linear changes, and that in fact, numerous factors may interact together and influence the records of deep-sea sediments in these complex regions of high productivity.

1.2.4 Sediment Regime

Site 1082 has a continuous sedimentary record based on density, magnetic susceptibility and colour reflectance data, spliced in small intervals from Holes 1082B and 1082C, where sediment column was disturbed or missed during the coring process. The 600 m long sediment sequence of Hole 1082A has well-developed cyclic sedimentation, with glacial and interglacial cycles represented as cycles of carbonate dissolution, productivity, and terrigenous sediment supply. Sediment is composed of continuous hemipelagic mud spanning the latest Miocene to Holocene (5.8 – 0 Ma), with the early-mid to late-Pleistocene, investigated in this study, composed of alternating intervals of bioturbated olive and black nannofossil- and foraminifer-rich clay (Jahn *et al.*, 2003). Varying abundances of diatoms, nannofossils, foraminifers, and radiolarians, and minor authigenic minerals, such as glauconite and gypsum, are found throughout the study interval (Wefer *et al.*, 2001).

Sedimentation rates are comparatively high within Leg 175 sites, varying between 70 to 150 m/myr (Durham *et al.*, 2001), Glacial-interglacial cyclicity of the late Quaternary is represented by cycles of carbonate dissolution, productivity, and terrigenous sediment supply, and is recorded as dark and light colour variations in the sediment retrieved from Site 1082. These colour cycles (total reflectance) reflect sharp changes in concentrations of calcium carbonate, organic carbon, and total sulphur. Generally, the darker layers have higher concentrations of organic carbon and total sulphur, and lower concentrations of calcium carbonate and biogenic opal (Wefer *et al.*, 1998). Changes in magnetic susceptibility down the core can also be utilized and reflect changes in terrestrial sediment input and calcium carbonate deposition across climatic cycles. At Site 1082, these well-developed cycles, in which concentrations of calcium carbonate

and organic carbon vary between 1 and 85% and <0.1 and 16.1 wt%, respectively, reflect fluctuations in the elevated marine production associated with the Benguela Current Upwelling System; higher concentrations of organic carbon recording higher productivities over the past 2 Ma (Wefer *et al.*, 1998). This high supply of organic matter drove intense diagenetic activity and periods of elevated carbonate dissolution. Studies by Berger (1970), Berger *et al.* (1982), and Emerson and Bender (1982), suggest that carbonate dissolution on continental margins in water depths above the oceanic lysocline or carbonate compensation depth (i.e. Site 1082) can only be attributed to decomposition of organic matter and resultant production of pore water CO_2. This dissolution is controlled by two processes: (a) surface water productivity (Berger, 1970) and (b) lateral supply of organic matter from the shelf and/or upper continental slope (Diester-Haass *et al.*, 1986). The equatorward movement of the South Atlantic high pressure system produced a similar shift in the upwelling-favourable Trade Winds (Tyson, 1986), strengthening of the coastal and shelf-edge wind field, and is thereby thought to have enhanced upwelling (intensity and increased productivity) along the Namibian margin during glacial and cooler interstadial periods.

The terrigenous input signal inferred from nearby Site 1081 reveals an increase in the supply of aeolian material during glacial periods (Durham *et al.*, 2001). In addition to increased supply of terrestrial material in response to the lowering of sea-level (global cooling and increased ice volume) and erosion of the now exposed continental shelf and slope areas, the strengthening of the coastal wind field during glacial intervals (and continental aridity) is inferred to have enhanced aeolian transport of sediment (including Fe and Si, recognized as having key roles in increasing primary productivity during glacial periods (Boyd *et al.*, 2004)) from the Namib desert into the region of the Walvis Ridge (Diester-Haass *et al.*, 1988). These two processes, an increase in surface water productivity and increase in the lateral supply of organic matter from continental shelf/upper slope areas, resulted in an increase in net organic matter accumulation and thus an enhanced carbonate dissolution during glacial times (Diester-Haass *et al.*, 1992). Ice-rafted debris (IRD) has not been encountered in previous studies as far north as Site 1082 (Siesser, 1980; Diester-Haass *et al.*, 1986, 1992).

1.3 *Southern Ocean sector of Southeastern Atlantic - Site 1088*

1.3.1 Regional Geology

Sites drilled during Leg 177 are associated with the Agulhas Basin and are arranged along a north-south transect extending from the Agulhas Fracture Zone Ridge in the north, to Bouvet Island in the south (Fig. 1.6). The Agulhas Basin lies on the African Plate and is bounded by the Agulhas Fracture Zone to the north, the Southwest Indian Ridge to the south, the Meteor Rise to the west, and the Agulhas Plateau to the east (Gersonde *et al.*, 1999).

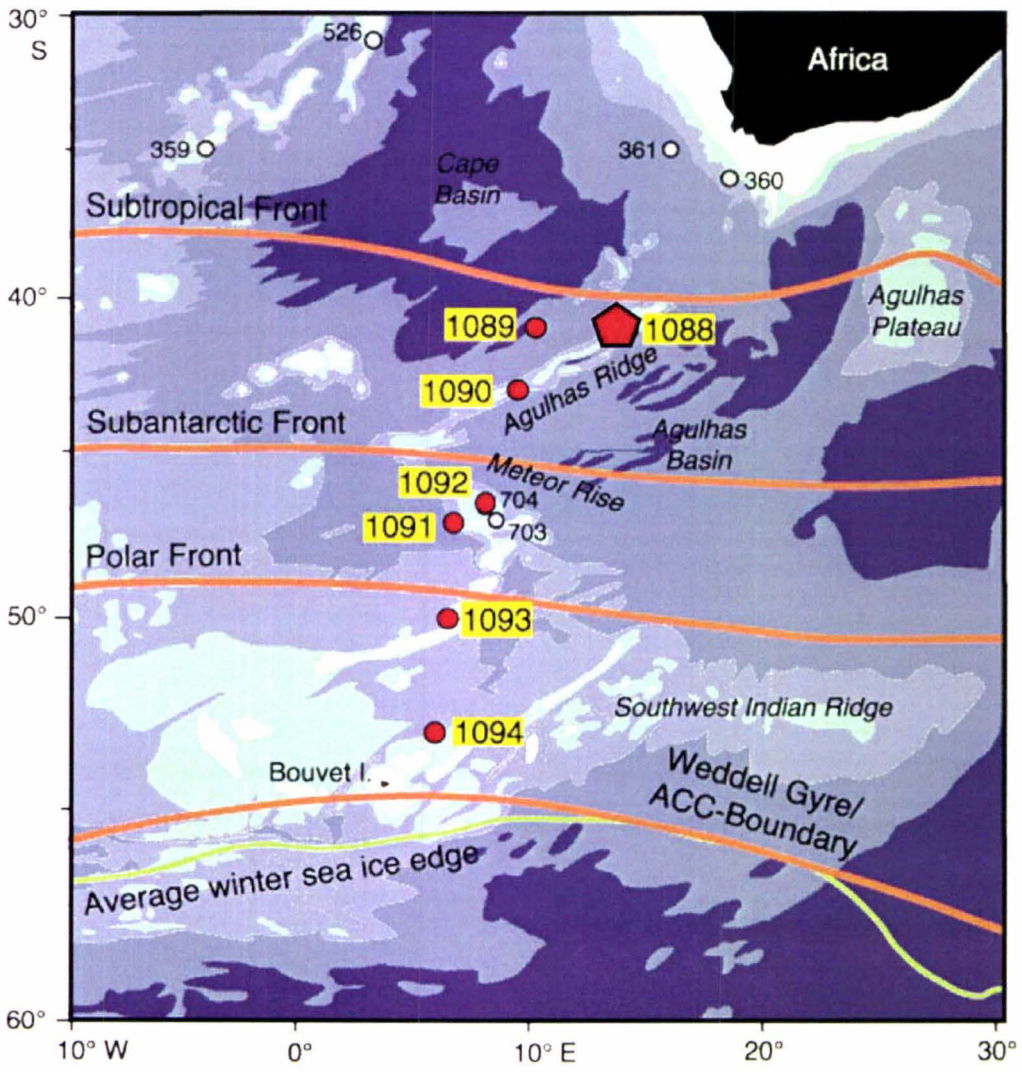

Figure 1.6: Location of Site 1088 in relation to other ODP Leg 177 sites (1088 - 1094), major bathymetric features and oceanic frontal boundaries (after Gersonde *et al.*, 1999) Note: The position of previous ODP sites in the Southern Ocean sector of the South Atlantic Ocean are also given.

The Agulhas Ridge is an elongate topographic feature that parallels the Agulhas Fracture Zone and extends from the northern tip of the Meteor Rise to terminate abruptly at 40°S, 15°E, where it intersects the northern end of an abandoned spreading-ridge axis in the Agulhas Basin (Gersonde *et al.*, 1999). Formation of the Agulhas Ridge is hotly debated; theories include formation from extension at the fracture zone resulting in serpentinite diapirism (Bonatti, 1978), and volcanic construction resulting from extension and/or a mantle plume, such as the Shona Hotspot (Kastens, 1987; Hartnady and le Roex, 1985). A thick sequence of pelagic mud covers the basement rocks of the Agulhas Ridge.

1.3.2 Location and Modern Oceanographic Setting

ODP Site 1088 (41.8°S, 13.3°E) was drilled during Leg 177 in 2082 m water depth on the broad northeastern end of the Agulhas Ridge, in the Southern Ocean sector of the South Atlantic Ocean, c. 700 km southwest of the tip of South Africa (Fig. 1.6).

The southeastern South Atlantic is an important component of the global conveyor circulation, representing the junction point of major ocean currents and the initial entry point of North Atlantic Deep Water (NADW) into the Southern Ocean. Site 1088 is located in the northern Subantarctic Zone between the Subtropical Front (STF) and the Subantarctic Front (SAF) (Fig. 1.6). This site is influenced by distal eddies and filaments of the Agulhas Current retroflection (Diekmann and Kuhn, 2002). Site 1088 is one of the shallowest of sites in ODP Leg 177 (well above the regional CCD) and is located at the boundary between upper Circum Polar Deep Water (CPDW) and North Atlantic Deep Water (NADW) (Fig. 1.7).

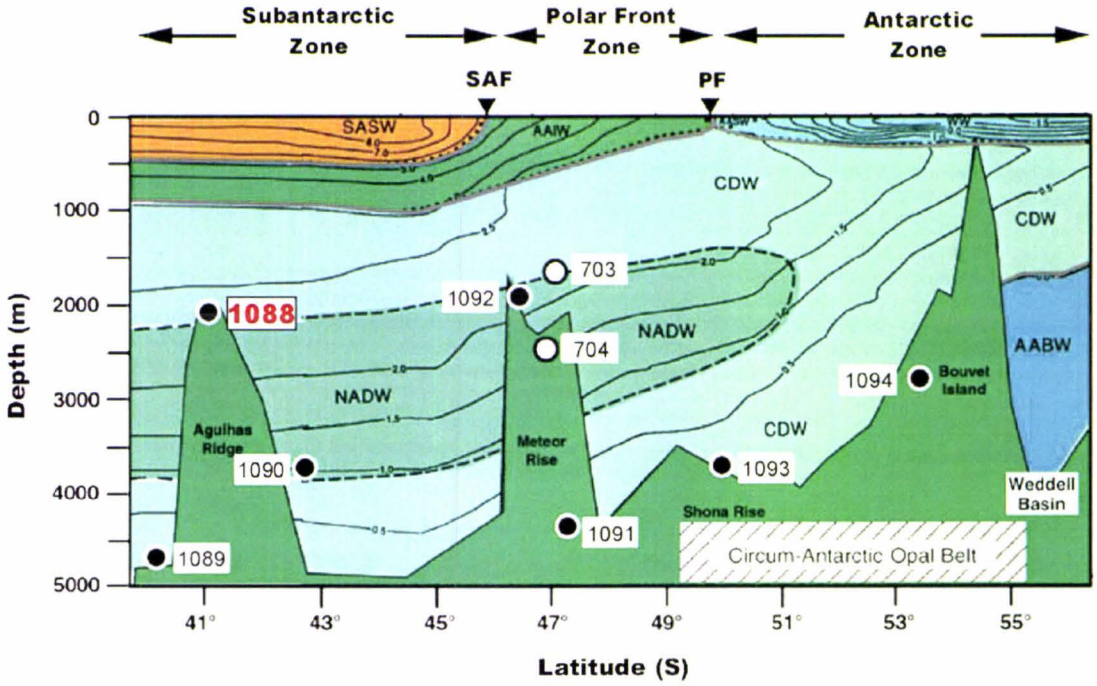

Figure 1.7: A cross-section of the present day intermediate- and deep-water masses, and frontal systems in the Southern Ocean sector of the South Atlantic Ocean, Site 1088 (modified from Gersonde *et al.*, 1999) AABW = Antarctic Bottom Water; CDW = Circum-polar Deep Water; NADW = North Atlantic Deep Water; AAIW= Antarctic Intermediate Water; SASW = South Atlantic Surface Water; SAF= Subantarctic Front; PF= Antarctic Polar Front

1.3.3 Past Oceanographic Changes

The unique location of Site 1088 gives great potential to reconstruct changes in the mean deep water mass composition over time, and elucidate past fluctuations in the production rate of Northern Component Water (NCW) (high latitude northern hemisphere sourced waters, such as the NADW), the strength of the NADW conveyor, and mixing ratios between NCW and Southern Component Water (SCW) (southern sourced waters, such as CPDW). Diekmann and Kuhn (2002) recognise two distinct modes of conveyor belt circulation in the study region during the MPT. The modern interglacial warm –route conveyor mode implies a far southward injection of relatively warm and saline NADW into the ACC, compensated to a large extent by the northward flow of warm surface and intermediate waters, which enter the South Atlantic via the Agulhas Current (Gordon *et al.*, 1992). The second mode of circulation occurred during glacial periods, when the cold-route conveyor mode is implied. This mode was characterised by prevailing cold southern-source water masses with a diminished NADW influx, in combination with only sporadic influence of the Agulhas Current leakage (Diekmann and Kuhn, 2002). These studies by Diekmann and Kuhn (2002) at nearby ODP Site 1090 revealed that glacial-interglacial contrasts in the regional

conveyor circulation strengthened across the MPT, roughly in accordance with global ice-volume fluctuations. Diekmann and Kuhn (2002) also inferred changes in deepwater circulation over the MPT using variations in sediment composition and clay mineralogy. Clay mineralogical studies revealed that Circumpolar Deep Water (CDW) expanded farther north during glacials after 1.2 Ma, further supporting the isotopic data of Venz and Hodell (2002)

1.3.4 Sediment Regime

Three holes were drilled representing a spliced record of 223.4 m, with the sediment investigated in this study, sampled between 5.39 and 14.38 mcd, being predominantly foraminifer-bearing nannofossil ooze (Gersonde *et al.*, 1999). Rock fragments interpreted as ice-rafted debris (IRD) occur at various frequencies down core. Site 1088 is situated northward of the Antarctic Polar Front (a zone centred at ~45°S with a latitudinal span of approximately ± 2.5° (Lutjeharms and Meeuwis, 1987)), such that glacial-interglacial migrations of this ecological and physical water mass boundary are unlikely to have had great influence on the biogenic sediment constituents at the site. Other than a slight shift in the area of dominant diatom deposition towards Site 1088, calcareous oozes, composed of calcareous phytoplankton (mainly coccoliths), calcareous zooplankton (mainly planktic foraminifera), form the biogenic component during both glacial and interglacial intervals (Diekmann *et al.*, 2003). Glacial-interglacial carbonate variations at Site 1088 are likely to be a result of dilution effects of biogenic and lithogenic sediment components, by changes in the mode of biological productivity and/or enhancement of terrestrial erosion and fluvial sediment supply during cold climate stages. During these stages, low stands of sea level facilitated glacigenic and fluvial sediment supply beyond the shelf and sediment gravity transport towards the deep sea. The water depth of < 3500 m places Site 1088 well above the regional lysocline, and thus the settling of calcareous particles is relatively unaffected by dissolution processes initiated by the glacial incursion of the corrosive CPDW. Furthermore, it has been inferred that improved carbonate preservation was likely at Site 1088 during the MPT, as slightly increased sedimentation rates (from 7 m/myr in the Pliocene, to 10 m/myr in the Pleistocene; Gersonde *et al.*, 1999) may promote survivability of calcareous particles.

Inorganic terrestrial sediment is sourced from the arid continental regions of South Africa and around the southern African margin, being supplied by the south-eastern trade winds, and to a lesser extent, through fluvial input and ocean currents. The latest findings from ODP Site 1090, which is situated to the west of Site 1088, have shown that fluctuations in illite chemistry (representing the major clay mineral from South Africa) are consistent with climatic oscillations in southern Africa (Diekmann and Kuhn, 2002). These studies reveal that abundant iron-bearing illite is indicative of arid conditions with prevailing physical weathering, typical of glacial intervals, whereas chemical weathering under humid interglacial conditions attacks and depletes iron-bearing illites and favours more stable Al-illites. Other significant studies, such as fluctuations in the ratio of kaolinite to chlorite, can be used to demonstrate changing source region of river particulates and latitudinal shifts in watermass boundaries. For example high kaolinite/chlorite ratios demonstrate Site 1088 was within the reaches of the Agulhas Current retroflection (Diekmann *et al.*, 2003).

A study of ice-rafted debris (IRD) delivery to the South Atlantic was undertaken by Kanfoush *et al.* (2000), in order to reconstruct the distribution of IRD across the PFZ. In the South Atlantic, IRD peaks reflect instability of ice shelves in the Weddell Sea region, and are associated with interstadial warm periods, and increased NADW production in the North Atlantic (Gersonde *et al.*, 1999) Kanfoush *et al.* (2000) revealed that the first identifiable IRD above background levels occurred at southerly ODP Site 1092 (~47°S) (Fig. 1.6) in the late Pliocene (~3.18 Ma), yet across the MPT there was no change in the amplitude or pacing of IRD delivered to the site. IRD has not been previously studied at Site 1088.

1.4 Previous Paleoceanographic Studies

1.4.1 Southeastern Atlantic Site 1082

The upwelling system associated with the Benguela Current is one of the most productive areas of the modern ocean, and as a consequence has been the focus of several studies into the evolution of upwelling and changes in productivity over geological time. Sediments from Deep Sea Drilling Project (DSDP) Sites 362 and 532 (1325 m and 1331 m water depth, respectively) (Fig. 1.1), which are close to Walvis Ridge ODP Sites 1081 and 1082, have provided a preliminary record of the evolution of upwelling and changes in biological productivity of the upwelling system.

Site 362 was rotary drilled during DSDP Leg 40 in 1975, resulting in all of the cores taken above a sub-bottom depth of 200 m being badly disturbed. Despite this, Siesser (1980) was able to conclude from changes in organic carbon and diatom abundances from Site 362 that upwelling-enhanced productivity had gradually increased since the onset of the Benguela upwelling system ~10 Ma (Miocene).

Hydraulic piston coring of Site 532 was undertaken in 1980, and yielded a more complete record of upwelling history (Hay and Brock, 1992). Peaks in concentrations of organic carbon and diatoms indicated that productivity also peaked at the Walvis Ridge location in the late Pliocene to early Pleistocene (Dean *et al.*, 1984). Further, Site 532 also revealed light-dark alternations in sediment colour, corresponding to changes in the concentrations of organic carbon, calcium carbonate, and clay minerals. Diester-Haass *et al.* (1986, 1992) conclude these colour changes record glacial-interglacial shifts of the Benguela Current, sea-level changes, oxidation strength, and source of terrigenous clastic sediment components.

Reconstructing the glacial-interglacial shifts in upwelling intensity were of high priority in studies by Durham *et al.* (2001). Preliminary investigations at ODP Sites 1081 and 1082 generally provide evidence for increased productivity during glacial periods. There is a prominent peak in all proxy records of productivity at 1100 ka that coincides with a maximum abundance of diatoms. This diatom abundance is observed in many records from the South Atlantic (Berger and Wefer, 1996) and is followed by a decrease

in abundance. Following this there is a rapid change in the dominant microfossil, with the abundance of foraminifera beginning to increase. The timing of these changes in productivity suggests that they may be related to the MPT.

The terrigenous input signal of the Walvis Ridge sites has also been a focus of previous study (Diester-Haass *et al.*, 1988). As expected, magnetic susceptibility records of Site 532 revealed increased terrigenous input during glacial periods in association with global cooling and enhanced aridity, leading to an increase in the supply of aeolian material. In the case of the Walvis Ridge location, aeolian transport from the Namib Desert by northeasterly to easterly winds was enhanced during glacial times (Durham *et al.*, 2001). In addition, Diester-Haass *et al.* (1988) suggested that the lowering of sea-levels in response to global cooling and increased ice volume during glacial periods, left greater areas of the continental shelf and slope exposed to erosion, which forms an important component of terrestrial input to Walvis Ridge sites. Studies by Diester-Haass *et al.* (1986) and Lutjeharms and Meeuwis (1987), revealed two contrasting terrigenous signals, one evident pre-MPT (prior to ~1200 ka), and another dominating the Walvis Ridge in the last 800 ka. Clay mineralogical evidence at DSDP Site 532 revealed that over the past 800 ka, supply of terrigenous material to the ridge has been a mix of reworked material from the continental shelf and material from the Orange River to the south, transported to the ridge by the intensified strength and flow of the Benguela Current during glacial periods (Lutjeharms and Meeuwis, 1987). In contrast, an opposite signal was evident in the pre-MPT period (prior to ~1200 ka), where mineralogy suggests increased terrigenous material during interglacial periods. This suggested that the supply of terrigenous material via aeolian input may have only been significant at the Walvis Ridge in the last 800 ka, implying that prior to this period a different source of terrigenous material played a major role. Further studies by Diester-Haass *et al.* (1986) revealed that the fluctuating position of the Angola-Benguela Front (ABF) (which controls the latitude at which the Benguela Current turns west, and the southerly extent of the southward-flowing Angola Current) (Fig. 1.3) influenced the source of terrigenous materials to the ridge. Kaolinite concentrations in interglacial sediments in the 1500 to 1000 ka period show a source of terrigenous material from the Kunene River, inferring that during this time the ABF may have been far enough south to allow supply and transportation to the Walvis Ridge via the Angola Current (Fig. 1.3). The timing of this change in supply and source of terrigenous input to the Walvis

Ridge coincided with the onset of the MPT. The associated increase in aridity of the African continent during this time may also have caused a decrease in the flow of the Kunene River (Durham *et al.*, 2001).

1.4.2 Southern Ocean sector Site 1088

Previous deep-sea drilling in the Southern Ocean include DSDP Leg 71 (Sites 511-514); ODP Legs 113 (Sites 689-697), 114 (Sites 698-704), 119 (Sites 739-746), and 120 (Sites 747-751), some of which are shown in figure 1.6. Sections recovered have provided a basic understanding of the paleoceanographic and paleoclimatic evolution of the southern high latitudes during the Cenozoic, but often core sections from previous Antarctic drilling are incomplete. Furthermore, cores are easily disturbed when recovered from the hostile seas of the Southern Ocean (Gersonde *et al.*, 1999). As a result of incomplete core recovery, disturbance, the presence of hiatuses, and diminished $CaCO_3$ preservation potential at high latitudes, efforts to obtain continuous paleoclimatic records in the Southern Ocean have been few and far between. Compared with the excellent records now available from the high-latitude North Atlantic Ocean, prior to Leg 177, the South Atlantic sector of the Southern Ocean had an obvious deficiency in the distribution of ocean-drilled cores, with relatively few continuous late Neogene records recovered. Of the 32 sites drilled during legs 113, 114, 119, and 120, only Site 704 (Leg 114) (Fig. 1.6) had sufficient stratigraphic continuity in the Plio-Pleistocene interval to allow for high-resolution paleoceanographic and paleoclimatic studies (Hodell and Venz, 1992). Thus, one of the primary aims during Leg 177 was to fill a critical gap in the distribution of drilled ocean sites to decipher the role the Southern Ocean had in the Quaternary history of the Earth's climatic system.

ODP Site 704 is positioned in the eastern Subantarctic South Atlantic (46°52.8'S, 7°25.3'E) (Fig. 1.6), within the mixing zone of the North Atlantic Deep Water (NADW) and Circum Polar Deep Water (CPDW), just north of the Antarctic Polar Front Zone (PFZ). The PFZ separates cold, nutrient-rich Antarctic surface water to the south from warmer, Subantarctic surface waters of lower nutrient status, to the north. Furthermore, the PFZ represents a transition zone from pure diatom ooze to the south near the Antarctic Polar Front to a mixed siliceous-calcareous ooze to the north near the Subantarctic Front (Hodell and Venz, 1992). Values of the $\delta^{18}O$ of precipitated calcite

demonstrate the PFZ is also a region of steep temperature gradients, and as a result, even subtle changes in the position of the PFZ can be recorded by the $\delta^{18}O$ of planktic foraminifers.

Isotopic data from Site 704 provided new insights into the climatic evolution of the Southern Ocean during the Plio-Pleistocene. Global climate is generally considered to have been warmer than today during the Pliocene (prior to 3.2 Ma), and the cryosphere is believed to have been unipolar and restricted to Antarctica (Hodell and Venz, 1992). During this time the amplitude of the planktic and benthic $\delta^{18}O$ signals was low (~0.5‰), accommodating some warming and minor deglaciation during the Pliocene. However, records are inconsistent with major warming and massive deglaciation of the Antarctic continent. Isotopic records from Site 704 suggest that the Antarctic glacier system did not fluctuate on a large scale prior to 3.2 Ma, rather, it was not until the late Gauss (2.7-2.4 Ma) (when the large Northern Hemisphere ice sheets developed), that the Southern Ocean underwent a major climatic transition. During this time faunal assemblages indicate the northwards advance of the PFZ and the accumulation of IRD in the Subantarctic sector. It is also thought that the lowering of sea level by increased ice in the northern hemisphere stimulated ice advance along the Antarctic margin. In addition, increased glacial suppression of NADW after 2.7 Ma may have decreased the heat flux to the Southern Ocean (Hodell and Venz, 1992). Carbon isotopic gradients between the North Atlantic (Site 607), the Southern Ocean (Site 704) and the Pacific (Site 677) suggest that the suppression of NADW intensified greatly during glacial periods after marine oxygen isotope (MIS) stage 52 (1.55 Ma), which in turn is attributed to an increase in the amplitude of the Earth's obliquity cycle (Hodell *et al.*, 2003).

Documentation of IRD, including Heinrich Events, in the North Atlantic has contributed greatly to our understanding of Laurentide Ice Sheet dynamics (Venz and Hodell, 2002). Kanfoush *et al.* (2000) found similar evidence for millennial-scale variability in the Antarctic Ice Sheet, through discrete episodes of IRD deposition throughout the last glaciation and over the last four climate cycles. The study of IRD delivery to the South Atlantic at Site 1094 (54°S) found that the last four glacial cycles were marked by high IRD abundance during the latter half of the interglacial period or onset of neoglaciation (composed predominantly of volcanic ash (source believed to be South Sandwich

Islands in the Scotia arc) and quartz with minor amounts of fine-grained volcanics, coarse-crystalline rock fragments, and mica); possibly reflecting the instability of the ice shelves in the Weddell Sea region (Venz and Hodell, 2002).

1.5 Mid-Pleistocene Climatic Transition

The mid-Pleistocene Climate Transition (MPT) is the name given to the period of time when the dominant periodicity of glacial-interglacial cycles changed from the 41-kyr obliquity signal to the 100-kyr eccentricity signal (Durham *et al.*, 2001). Broecker and van Donk (1970) described it as the transition observed in proxy climate records from symmetrical low-amplitude, high-frequency (41-kyr) ice volume variations to high-amplitude, low-frequency (100-kyr) asymmetrical saw-toothed ice volume variations indicating gradual ice build-up terminated by rapid deglaciation events. During the MPT, glacial-interglacial contrasts became more severe and the 100-kyr climate cycles developed their distinctive asymmetric pattern of the late Quaternary, resulting in a change in the mean state of the global climate system, including lower global temperatures, increased global ice volume, and lower sea-surface temperatures (Shackleton *et al.*, 1990).

The MPT occurred over several hundred thousand years (between c. 1200 and 600 ka) and is documented by benthic foraminiferal $\delta^{18}O$ records in marine sediments from the world's oceans. Benthic foraminiferal $\delta^{18}O$ records document a general increase in global ice volume and the onset of weak 100-kyr cycles between 1250 ka and 900 ka and the establishment of strong 100-kyr cycles since 600 ka (Ruddiman *et al.*, 1989; Imbrie *et al.*, 1993; Berger *et al.*, 1994; Chen *et al.*, 1995; Mudelsee and Schulz, 1997). Ruddiman *et al.* (1989) and Mix *et al.* (1995) report a benthic $\delta^{18}O$ increase of approximately 0.29‰ at ~920 ka, which corresponds to a sea level fall of about 30 m.

During the same time interval significant changes in carbon cycling was occurring, including changes in the mean ocean $\delta^{13}C$, probably caused by the addition of terrestrial carbon to the ocean-atmosphere reservoirs as global aridity increased (Raymo *et al.* 1997). Positive feedbacks to the CO_2 budget on earth, an increase in carbon in the marine realm (from increased primary production and transport from continental shelf to deep sea), along with many other factors, are thought to have affected deep-water physical and chemical composition in the North Atlantic (NADW) and subsequently the global thermohaline circulation of the oceans.

The timing, duration, and the cause of the MPT is yet to be adequately explained. It is, however, known that the MPT was a global event, and its occurrence has been well documented in both marine and continental records worldwide. The problem lies in identifying a mechanism that would amplify the climate system's response to relatively weak insolation forcing. The MPT demonstrates that the causal link between insolation and ice volume suggested by Milankovitch (1930) is, in fact, much more complex than it may first appear. During the Pliocene and early Pleistocene it appears that a linear relationship between orbital forcing, ice volume and climate variations existed (Imbrie *et al.* 1993). Yet, reconstructions of insolation values by Berger and Loutre (1991) suggest that there is no significant change in the pattern of insolation at the time of the MPT to account for the transition observed in climatic variations from 41- to 100-kyr cycles. The lag between ice growth at 920 ka and the establishment of strong 100-kyr world at ~650 ka, further complicates the problem, indicating decoupling between ice volume and the 100-kyr cycle.

1.6 Previous Studies on the Extinction of deep-sea Benthic Foraminifera

1.6.1 Cenozoic Turnover of Benthic Foraminifera

Three periods of increased taxonomic turnover and in faunal abundance changes in deep-sea foraminifera during the Cenozoic have been identified globally (Thomas, 1992; Miller *et al.*, 1992): the Paleocene-Eocene boundary, Eocene-Oligocene boundary, and middle Miocene. Of these, the first, resulted in the most severe extinctions of benthic foraminifera (loss of 30-50% of species; Thomas, 1992; MacLeod *et al.*, 2000) during the Paleocene-Eocene thermal maximum (PETM, ca. 55 Ma). This extinction has been attributed to an abrupt warming and change in ocean circulation due to circulation of oxygen-poor, warm, corrosive bottom waters, coupled with changes in primary productivity in the surface waters (Katz *et al.*, 1999). The second and third periods of increased taxonomic turnover the 36-30 Ma and 16-12 Ma were more gradual, correlating with a decrease in high latitude and deep-water temperatures (Shackleton and Kennett, 1975; Thomas, 1992), and a shift in $\delta^{13}C$ values (initiated by changes in surface ocean productivity), respectively.

1.6.2 Mid-Pleistocene Extinction of Benthic Foraminifera

The mid-Pleistocene extinction or "*Stilostomella* extinction event" (Weinholz and Lutze, 1989) has now been recognised as the most recent turnover in benthic foraminiferal taxa. First documented in DSDP Site 397 off north-west Africa in the Atlantic Ocean (Lutze, 1979), it marks the final phase in the progressive decline of elongate cylindrical taxa (belonging to the families Stilostomellidae, Pleurostomellidae and uniserial Nodosariidae). It includes the extinction of all elongate, cylindrical, uniserial, biserial or multiserial tests with highly specific apertural characteristics: i.e. cribrate (*Chyrsalogonium, Cribronodosaria*), slit lunate, hooded with two teeth (Pleurostomellidae), or secondarily toothed, necked (Stilostomellidae) apertures (Hayward, 2002). These fauna reached their greatest abundance (up to 70% of benthic foraminiferal faunas) in the latest Eocene (40-35 Ma), forming a significant proportion of middle bathyal to upper abyssal (c. 500-3000 m depth) benthic foraminiferal faunas (Thomas *et al.*, 2000). Since the latest Eocene this group of elongate taxa has

progressively declined in abundance and diversity, with strongest declines occurring during the late Eocene-early Oligocene cooling when the East Antarctic Ice Sheet formed (Thomas and Vincent, 1987), and the late middle Miocene cooling, related to the expansion of the West Antarctic Ice Sheet (Thomas 1987, 1992). The final demise of the Extinction Group taxa, called the "*Stilostomella* extinction", reported here, occurred between 1000 and 600 ka (Lutze, 1979; Weinholz and Lutze, 1989; Schönfeld, 1996), and has been hypothesized to be related to the intensification of Northern Hemisphere glaciation, and associated changes in the oxygenation of bottom-water masses and food supply fluctuations.

Figure 1.8 illustrates the global locations of deep-sea ODP and DSDP sites in which the "*Stilostomella* extinction" event has previously been documented. Lutze (1979) identified the decline and extinction of 10 benthic foraminiferal species from six genera (e.g. *Stilostomella, Orthomorphina, Plectofrondicularia, Ellipsoglandulina, Nodogenerina,* and *Pleurostomella*) between 1000 and 600 ka in DSDP 397 off northwest Africa in the Atlantic Ocean.

When Weinholz and Lutze (1989) undertook a detailed investigation of DSDP 658 and 659, off west Africa they initiated the term "*Stilostomella* Extinction", named after the family Stilostomellidae which disappeared at this time; which has been used since to describe this global benthic foraminiferal extinction event. Their study revealed the diachronous nature of the faunal boundary, with highest occurrence datums (HOs) of the Extinction Group taxa spanning some two hundred thousand years (810 - 640 ka), the timing differing between sites and water depth. An important discovery made by Weinholz and Lutze was that the final extinction of the taxa appeared to be c. 100 kyr earlier in the deeper water (DSDP 659, 3081 m) than shallower (DSDP 658, 2263 m).

Gupta (1993) then confirmed the decline in relative abundance and eventual demise of *Siphonodosaria lepidula* (as *Stilostomella lepidula*) in the Pliocene and Pleistocene of two DSDP sites (DSDP 214 and 219) in the Indian Ocean. Benthic census data showed a progressive decline in relative abundance of *Siphonodosaria lepidula*, from greatest abundance during the late Pliocene (3.2-1.8 Ma), comprising 10-20% of the benthic foraminiferal fauna >150 μm, to an abrupt decrease and regional disappearance at ~ 730 ka, near the Brunhes/Matuyama boundary (780 ka).

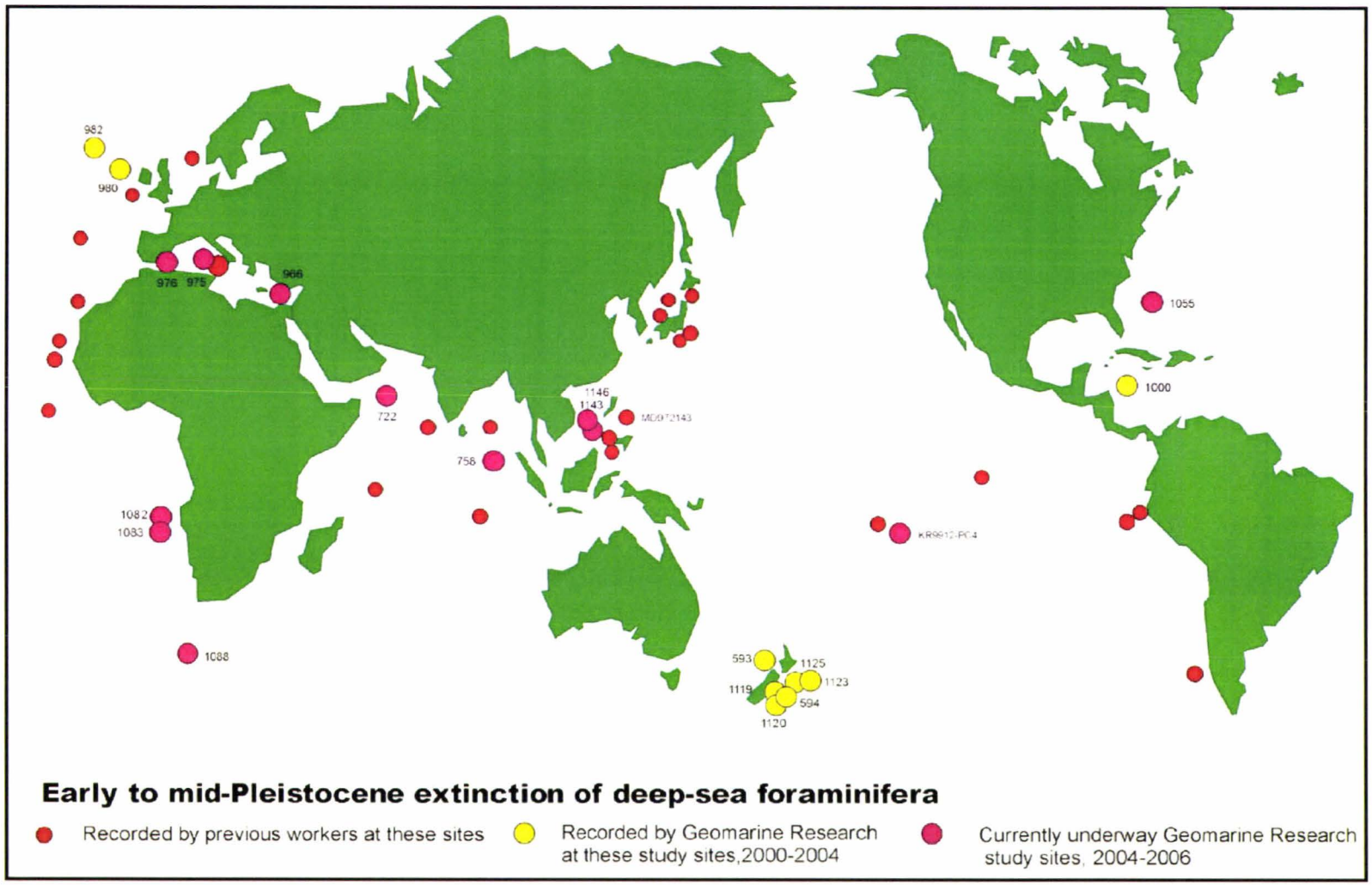

Figure 1.8: Global location of ODP and DSDP sites in which the "*Stilostomella* extinction" has previously been documented (modified after Hayward, 2002).

In the Pacific Ocean the "*Stilostomella* extinction" has been recognised in the northwest (Kaiho, 1992; Keller, 1980; Jian *et al.*, 2000), central (Schönfeld, 1995), southeast (Schönfeld and Spiegler, 1995) and southwest (Hayward, 2001, 2002).

Schönfeld (1996) reviewed all known records of the mid-Pleistocene extinction event, which confirmed the extinction (HOs) of the relevant species of elongate benthic foraminifera between 1000 and 600 ka (predominately 800 to 700 ka) with highly variable timings. He noted the diachronous nature of highest occurences in sites only a few tens or hundreds of kilometres apart, e.g. DSDP 658 and 659, or 548 and 549, in the Central and North Atlantic Ocean, with HOs of *Siphonodosaria lepidula* differing by 166,000 and 155,000 years respectively (Schönfeld, 1996). Schönfeld also concluded that regional extinctions took place earlier in water depths below 3500 m, farther offshore, and at mid- to low southern latitudes, possibly linking rapid changes in deep-water formation and ventilation with the "*Stilostomella* extinction".

Hayward (2001, 2002) undertook the first detailed "*Stilostomella* extinction" study which included the decline and extinction of the rare and small taxa (>63 μm), which had been overlooked in most previous studies. Hayward (2002) revealed that in the southwest Pacific, the total abundance of Extinction and Die-back Group specimens decline dramatically during the early and middle Pleistocene (1200-700 ka), the rate of decline is not uniform but pulsed, often with major declines coinciding with the onset of cold intervals. Further, Hayward (2002) concluded that in the southwest Pacific, the local disappearances of the Extinction Group species occurred earlier in deeper and cooler water locations (earliest site ODP 1123 and latest site ODP 1125), suggesting the pattern may be related to food supply. Contrary to Schönfeld's conclusion of highly variable youngest occurrence timings of the Extinction Group taxa (900-600 ka, Schönfeld, 1996), Hayward's southwest Pacific sites revealed a highly consistent final disappearance of the taxa, constraining the *Stilostomella* extinction datum to 650-570 ka, despite differences in depth.

Most recently, Kawagata *et al.* (in press) document the extinctions of deep-sea benthic foraminifera in the North Atlantic Gateway. ODP Sites 980 and 982, located in intermediate water depths in the northern North Atlantic, are close to the present formation area of North Atlantic Deep Water (NADW). Both cores reveal the

progressive decline and eventual regional extinction of 51 species of elongate, cylindrical benthic foraminifera, with the majority of Extinction Group taxa (~96%) having HOs between 1200 and 700 ka. The last of these species to disappear in the North Atlantic was *Pleurostomella alternans* at ~679 ka and ~694 ka in Sites 980 and 982, respectively. These North Atlantic studies are in good agreement with the previously documented final global "*Stilostomella* extinction" datum of 700-580 ka (Weinholz and Lutze, 1989; Kaiho, 1992; Gupta, 1993; Schönfeld, 1996; Hayward, 2001, 2002). They concluded that changes in chemical ventilation of the bottom water and food supply to the sea floor might have decimated the elongate, uniserial deep-sea foraminifera during the MPT.

1.7 Marine Oxygen Isotope Stages

The Milankovitch theory of climate change, linking variations in the Earth's orbital parameters to climate fluctuations, continues to gather support as the primary driver for glacial and interglacial climatic cycles. Much of the climatic cyclicity that is documented in the marine sedimentary record over the past 1 million years can be explained by linear responses of climate to the 41,000-year orbital obliquity and 23,000-year orbital precession cycles. The increasing availability of long, high quality ODP cores has made it possible to monitor spectral signals and phase relationships back beyond the Miocene. However, orbitally modulated fluctuations of solar irradiance alone cannot explain the longer-term evolution of the Earth's climate system. An important component in the long-term Cenozoic cooling trend was plate tectonics, namely its influence on mountain uplift and ocean circulation. There is now abundant evidence that the reconfiguration of oceans and continents, notably the opening and closure of oceanic gateways, and associated change in thermohaline circulation and heat transport, set the stage for northern hemisphere glaciation (Imbrie *et al.*, 1993). Thermohaline forcing through changes in deep water temperature has been proposed by Imbrie *et al.* (1993) to be one possible driver of the 100,000-year climate cycle. Further studies involving high-resolution correlations between ice core paleoclimate records and the marine $\delta^{18}O$ record support not only a dominant greenhouse forcing (Shackleton, 2000), but also reveal a lag period between ice volume (as seen in the marine record) and atmospheric CO_2 changes. Such evidence favours atmospheric CO_2 as the primary player during the long-term cycles of glacial-interglacial climatic change (Shackleton, 2000).

The marine oxygen isotope stage numbering system that is used throughout this thesis is based upon the timescale calibrated by Chen *et al.* (1995), for the 0-1.8 Ma period (Fig. 1.9). Chen *et al.* (1995) use the $\delta^{18}O$ records from the benthic foraminiferal species *Cibicides wuellerstorfi* to simulate orbitally-induced ice volume changes over the past 3.6 Ma (ODP 758). The marine isotope stages (MIS) are recognised in the glacial and interglacial periods based on the downcore variation of the $\delta^{18}O$ of foraminifera and are labelled using conventional notations of even numbers for glacial stages and odd numbers for interglacial stages.

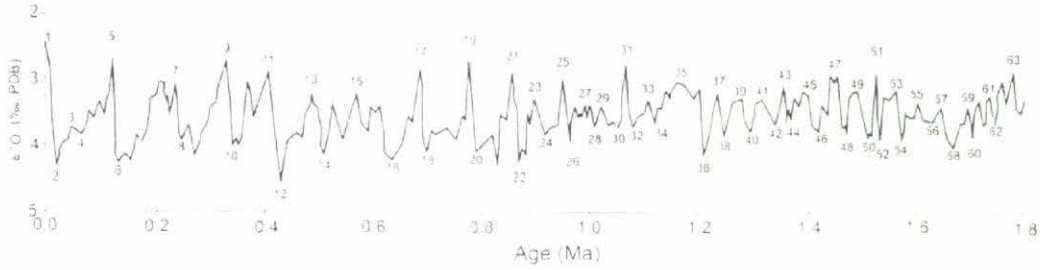

Figure 1.9: Calibrated ages for marine isotope stages (MIS) for last 1.8 Ma, using ice volume simulation (*from* Chen *et al.*, 1995).